PEGylated Versus Non-PEGylated γ Fe2O3@Alendronate Nanoparticles

Benyettou F, J Hardouin, Marc Lecouvey, H Jouni, Motte L

Journal of Bioanalysis & Biomedicine

Benyettou et al., J Bioanal Biomed 2012, 4:3
DOI: 10.4172/1948-593X.1000062

Research Article Open Access

PEGylated Versus Non-PEGylated γFe_2O_3@Alendronate Nanoparticles

Benyettou F, Hardouin J, Marc Lecouvey, Jouni H and Motte L*

Laboratoire CSPBAT UMR CNRS 7244, Université Paris 13, 74 Rue Marcel Cachin, 93017 Bobigny France

Abstract

Thanks to their magnetic properties, superparamagnetic iron oxide nanoparticles are considered as a good delivery vehicle after grafting a therapeutical drug on their surface. For additional "stealth" characteristics, PEGylation of surfaces is necessary. The presence of PEG chains divert nanoparticles from their preferred target, the liver macrophages and increased the particle time circulation.

In this work, PEG chain is added to an anticancer drug Alendronate. This molecule is grafted on iron oxide nanoparticle surface in one step surface functionalization method. The *in vitro* cytotoxic efficiency of γ-Fe_2O_3-Alendronate-PEG nanocrystals is compared with that of free Alendronate, Alendronate-PEG and γ-Fe_2O_3-Alendronate nanocrystals.

Keywords: Magnetic nanoparticle; Alendronate; Anticancer drug; Polyethylene glycol; Nanocarriers

Introduction

In previous work, we have designed new antitumor magnetic nanoparticles by coating iron oxide nanoparticles with a clinically relevant antitumor agent: alendronate [1]. We show that these nanoparticles have both MRI contrast agent and anti-cancer properties. This nanoparticle functionalization spectacularly improved Alendronate cell penetration and its antitumor effect. In particular, this behavior was enhanced in the presence of an appropriate magnetic field [2,3]. In vivo experiments confirmed the therapeutic efficacy of γFe_2O_3@alendronate nanocrystals in the presence of a magnetic field [1]. The particles, loaded with the drug, were concentrated at the target site by an external magnet. However, for relevant drug delivery, we explored the addition of PEG chains on the γFe_2O_3@alendronate nanocrystals (Figure 1). PEG is a biocompatible polymer that has both hydrophilic and hydrophobic properties [4-6]. Chemically grafted or simply adsorbed on a colloid surface, it reduces the proteins adsorption [7,8] and bacterial adhesion [9]. This anti-adhesive effect is correlated to its high affinity for water molecules, which creates on the particle surface a layer highly hydrated making the adhesion of macromolecules very hard [10]. The presence of PEG chains will permit to divert nanoparticles from their preferred target, the liver macrophages [11]. Thanks to their molecular mobility, PEG chains push the opsonins by steric repulsion process and prevent them from binding to the surface of the nanocarriers, which, therefore, are no longer recognized by the liver and the spleen. In vivo, this translates into a decrease in interaction with proteins of the serum and increased the particle time circulation [12]. Moreover, unlike to vascular membranes of safe tissue, pathological tissues are more permeable due to the inflammatory reaction caused by the tumor (EPR effect). By increasing the nanoparticle lifetime in plasma, it increases their accumulation in the tumor and makes them release the active drug [13]. The presence of the polymer at the surface can also stabilize particles, avoiding their aggregation; reduce the surface charge and interactions with cell [14-16] (Figure 1).

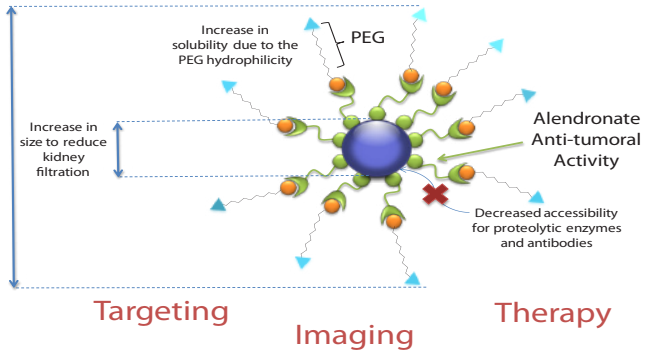

Figure 1: Schematic representation of the γFe_2O_3@alendronate-PEG nanoplatform nanoparticle.

The aim of this study is to present the elaboration and *in vitro* evaluation of PEGylated γFe_2O_3@alendronate nanocrystals. For the elaboration of PEGylated γFe_2O_3@alendronate nanocrystals, we synthesized a new bisphosphonate (Figure 2) that will have both therapeutic properties with the presence of Alendronate and PEG chains.

This new nanoplatform is characterized by various physicochemical methods and the cytotoxicity of the surface modified nanoparticles has been assessed on two cell line models (Human umbilical vein endothelial cells as human normal cells and MDAMB-231 breast human as cancer cell line) using standard 3-(4,5-dimethylthiazol-2-yl)-2,5-diphenyltetrazolium bromide (MTT) assay. A comparison between pegylated and non pegylated nanoplatforms is presented.

Materials and Methods

Synthesis of γFe_2O_3 @alendronate and γFe_2O_3 @alendronate-PEG nanocrystals

Synthesis of uncoated γFe_2O_3 particles was already described [1,3]. A solution of dimethylamine 40% in water ($(CH_3)_2NH$, 10^{-5} mL) is added

***Corresponding author:** Motte L, Laboratoire CSPBAT UMR CNRS 7244, Université Paris 13, 74 Rue Marcel Cachin, 93017 Bobigny France, E-mail: laurence.motte@univ-paris13.fr

Received April 04, 2012; **Accepted** May 08, 2012; **Published** May 12, 2012

Citation: Benyettou F, Hardouin J, Lecouvey M, Jouni H, Motte L (2012) PEGylated Versus Non-PEGylated γFe_2O_3@Alendronate Nanoparticles. J Bioanal Biomed 4: 039-045. doi:10.4172/1948-593X.1000062

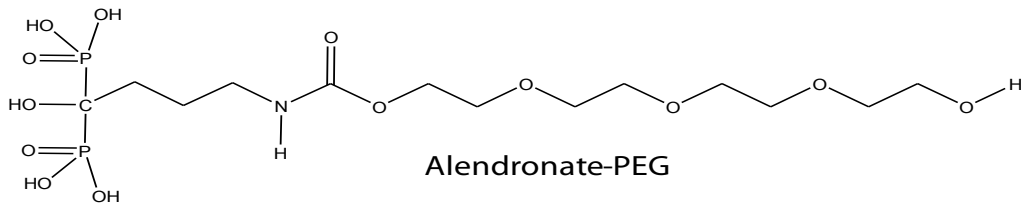

Figure 2: Chemical structure of Alendronate-PEG: [1-Hydroxy-4-(2-{2-[2-(2-hydroxy-ethoxy)-ethoxy]-ethoxy}- ethoxycarbonylamino)-1-phosphono-butyl]-phosphonic acid.

to an aqueous micellar solution of ferrous dodecyl sulfate ($Fe(DS)_2$) (0.61 g, 10^{-3}mol). The solution is stirred vigorously for 2 h at 28.5°C and the resulting precipitate of uncoated nanocrystals was isolated from the supernatant at pH=7 by magnetic separation and washed with an acidic solution (HCl 10^{-1} mol.L^{-1}). The average size of the particle is 10 nm in diameter (see TEM micrograph and size distribution SI). A solution of alendronate or alendronate-PEG molecules (n=10^{-4}mol in 30 mL of water) was added [3,17,18] to the colloidal suspension. The mixture is stirred for two hours at room temperature. The precipitate is washed with an acidic solution (HCl 10^{-1}mol.L^{-1}). Free alendronate were isolated from the coated particles thanks to a magnetic field and by centrifugation (3000T/min). Free alendronate-PEG molecules were removed by dialysis. The magnetic nanocrystals coated with alendronate or alendronate-PEG molecules are dispersed in water. The pH was increased to 7.4 by addition of sodium hydroxide (NaOH 10^{-1}mol.L^{-1}). Iron concentration was deduced from ultraviolet-visible absorption.

Nanoparticles characterization

Transmission electron microscopy (TEM): The average nanoparticle size was determinate with TEM. Samples were prepared by drying a drop of a dilute aqueous solution of γFe_2O_3 nanocrystals onto a carbon coated copper grid. TEM analysis was then carried out on a Philips CM10.

UV-Visible spectrophotometry: The iron concentration of the various samples was deduced from UV-visible absorbance spectroscopy experiments (Varian Cary 50 Scan UV-Visible spectrophotometer). Beer-Lambert law was used at 480 nm.

Infrared spectroscopy (IR): In order to qualitatively characterize the binding of molecules onto the surface of the γFe_2O_3 nanocrystals via phosphonate groups, IR analysis was performed using a Thermo Electron Corporation Nicolet 380 IR spectrometer.

Nuclear magnetic resonance (NMR) spectroscopy: The average number of molecules per nanocrystal is deduced with ^{31}P NMR spectroscopy [1,17] using a Varian Gemini spectrometer (200 MHz) and scanned in the range of 0-20 ppm. A range of concentrations of free Alendronate (NMR 31P {1H} (80.9 MHz): 17.076 ppm) and free Alendronate-PEG (NMR ^{31}P {1H} (80.9 MHz): 17.2 ppm) solutions added with an internal reference NaH_2PO_4 (in capillary, 10^{-1}mol.L^{-1}; NMR ^{31}P {1H} (80.9 MHz): 0 ppm) was prepared for calibration. After chemical decomposition of the magnetic γFe_2O_3@alendronate and γFe_2O_3@alendronate-PEG nanocrystals in acidic medium (nitric acid 65%), the ferrous ions were precipitated by addition of sodium hydroxide NaOH (10^{-1} mol.L^{-1}) in order to avoid shifting of the ^{31}P NMR signal. The supernatant containing the free molecules of bisphosphonates was then analyzed with ^{31}P NMR (in capillary[NaH_2PO_4] = 10^{-1} mol.L^{-1}) and the concentration (number of molecules per nanocrystal) of alendronate and alendronate-PEG into the sample was deduced from this calibration plot.

Dynamic light scattering (DLS): DLS measurements were achieved using a Nano-ZS (Red Badge) ZEN 3600 device (Malvern Instruments, Malvern, UK) giving size and ξ potential evaluations. Diluted ferrofluid ([Fe] = 5.10^{-4} mol.L^{-1}) at pH = 7.4 were used for the measurements of the hydrodynamic diameter and zeta potential, with Nano-ZS device.

In vitro studies

Cell lines and culture: Human umbilical vein endothelial cells (HUVEC) from PromoCell (Heidelberg, Germany) were cultured in Endothelial Cell Growth Medium supplemented with supplements and growth factors containing hydrocortisone, hEGF, FBS, VEGF, hFGF-B, R3-IGF-1, ascorbic acid, heparin and gentamycin/ amphotericin-B. Carcinoma cells line (MDA-MB-231) from American Type Culture Collection were cultured in Dulbecco's modified Eagle's medium (DMEM) supplemented with 10% calf serum, 2 mM L-glutamine, 1 mM sodium pyruvate, 50 U/ml streptomycin (all obtained from Life Technologies Inc.), at 37 °C in a 5% CO_2 humidified atmosphere. All *in vitro* cell experiments were carried out at 37°C in a 5% CO_2 incubator.

In vitro cytotoxicity assay

Cell viability was evaluated using the MTT microculture tetrazolium assay 26 based on the ability of mitochondrial enzymes to reduce 3-(4,5-dimethylthiazol-2-yl)-2,5-diphenyltetrazolium bromide (MTT) (Sigma, St. Louis, Mo) into purple formazan crystals. Cells were seeded at a density of 104 cells per well in 96-well flat-bottom plates (Falcon, Strasbourg, France) and incubated in completed culture medium for 24 h. Then, for MDA-MB-231, and HUVEC cells, medium was removed and replaced with medium containing increasing concentrations of different formulation of alendronate and alendronate-PEG from 100 µM to 1.6 µM. After 48 h incubation, cells were washed with phosphate buffered saline (PBS, Life Technologies) and incubated with 0.1 ml of MTT (2 mg/ml, Sigma-Aldrich) for additional 4 h at 37°C. The insoluble product was then dissolved by addition of 100 µl of DMSO (Sigma-105 Aldrich). The absorbance corresponding to the solubilized formazan pellet (which reflects the relative viable cell number) was measured at 540 nm using a Labsystems Multiskan MS microplate reader. The measurement was performed on DMSO solubilized formazan pellet using PBS washed cells as blank control. Dose-response curves were obtained for all suspensions, allowing the determination of IC_{50} values, half maximal inhibitory concentration. It is a characteristic measure of the effectiveness of a compound in inhibiting biological or biochemical function. All in vitro experiments had been done in triplicate.

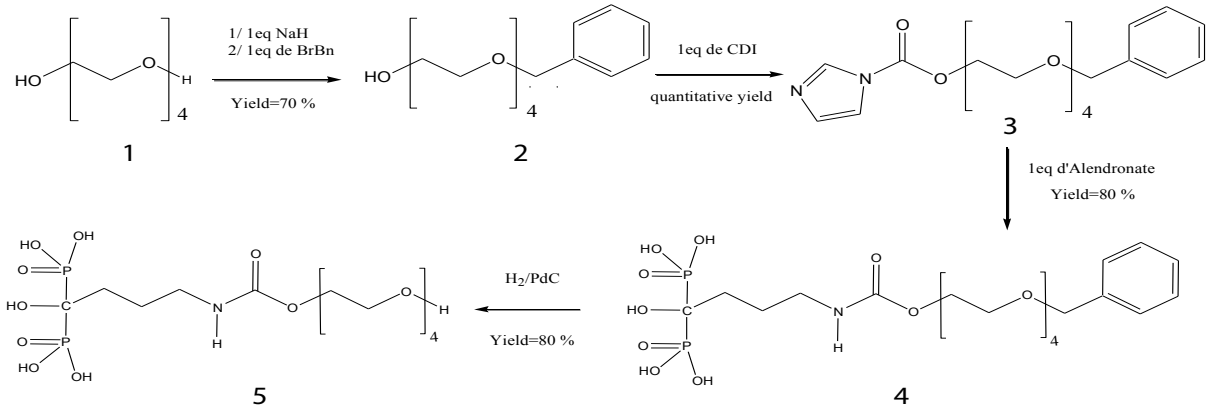

Figure 3: Synthetic scheme of Alendronate-PEG synthesis.

	Amine I(N-H)	-CH_2(C-H)	Phosphonate(P=O, P-OH,P-OM)	Fer-xygène(Fe-O)
Alendronate	1524	1473	1168 1073 913	-
γ-Fe_2O_3-Alendronate nanocrystals	1524	1471	1110 1057 1001	569

	Amide (C=O)	Amide (N-H)	-CH_2(C-H)	Alcohol-OH	Phosphonate (P=O, P-OH, P-OM)	Fer-Oxygen (Fe-O)
Alendronate-PEG	1701	1541	1458	1350	1138 1095 915 886	-
γ-Fe_2O_3-Alendronate-PEGnanocrystals	1697	1540	1456	1352	1091 1024 972	580

Table 1: Characteristic Infrared vibration bands for Alendronate and Alendronate-PEG molecules free or grafted on γFe_2O_3 nanocrystalsurface.

Results and Discussion

Synthesis of a new bisphosphonate: Alendronate-PEG

The Alendronate-PEG (**5**), is obtained by covalently coupling alendronate molecule (4-Amino-1-hydroxy-1-phosphonobutyl) phosphonic Acid) with polyethylene glycol 200 (**1**) through a carbamate linkage [19] (Figure 3). The synthesis procedure of precursor molecules and chemical characterization is described in supporting information. The synthesis is performed in four steps. Firstly, one hydroxyl functions of PEG (1) is protected by a benzyl protecting group reacting one eq. of sodium hydride (NaH) with one eq. of PEG **1** . The resulting benzylalcohol **2** is activatedin the presence of 1.1 eq. of CDI (1,1 '-carbonyldiimidazole) to give the imidazol derivative which can undergo nucleophilic displacement reaction in the presence of alendronate in basic conditions **3.** The addition of alendronate amino form allows the carbamate bond formation and the coupling product **4** was obtained in 80% yield. In the last step, deprotection of benzyl group of Alendronate- PEG **4** was carried out by hydrogenolysis**.** The Alendronate-PEG **5** was obtained in 45% overall yield.

Nanoparticle characterization

Stability and size measurements: Figure 4 shows a TEM photograph and size distribution of nanoparticles after grafting of (A) Alendronate and (B) Alendronate-PEG molecules on nanoparticle surface. In both cases, size distribution are quasi-homogeneous giving a mean diameter of 10 nm and a polydispersity index 0.2 (log normal distribution) as well as uncoated particles [1,3]. The particles are relatively spherical in shape and more or less agglomerated.

The colloïdal behavior of γFe_2O_3@alendronate and γFe_2O_3@ alendronate-PEG nanocrystals was determined by dynamic laser light scattering (DLS) (Figure 5). Surface charge is a major determinant of solution stability, susceptibility to aggregation and precipitation problems, as well as of protein and cell-surface binding in vivo [20,21]. Considering surface functionalization with alendronate molecules, ferrofluid are stable between 4 to 12 pH range. In this pH domain stability, nanoparticles exhibited an increasing negative zeta potential. The negative surface charge has to be considered in the light of alendronate charges: indeed, these molecules are highly charged, with five 5 pKa values (≈0.8, 2.2, 6.3, 10. P-OH/PO^-, and 12.2 NH_3^+/ NH_2). HMBPs coordinate to iron surfaces via two Fe-O-P bonds (corresponding to pKa_1 and pKa_2), and therefore at pH 7.4, the negative charge is due to the third deprotonated hydroxyl group. Hence, coating with alendronate made the solution anionic. This is well illustrated by

the zeta potential for bare and alendronate-coated nanoparticles as a function of pH (Figure 5). The surface charge was dependent on the coating. The isoelectric point (IEP) of γFe_2O_3@alendronate was about 4.7, and was thus shifted to acidic pH values relative to that for bare nanoparticles. The efficiency of the coating was thereby confirmed by the displacement of the isoelectric point of the nanoparticles as well as by the zeta potential as a function of pH. The mean crystalline core is 10 nm in diameter but at pH=7 the hydrodynamic size is around 32 nm suggesting few aggregates due to a lack of charge at this pH [1,17].

With Alendronate-PEG molecules as surface coating agent, the stability domain extend between 2 to 12 (Figure 6). Moreover, the zeta potential (Figure 5A black curve) as well as hydrodynamic size (Figure 5 B black curve) of $\gamma Fe_2O_{3@}$alendronate-PEG nanocrystals are nearly constants, 2 mV and 15 nm respectively. The quasi neutral charge could be due to hydroxyl terminal end group of PEG (pKa =16) whereas the PEG chain length favors steric repulsion between particles, reducing aggregation state. Hence, the efficiency of the coating was thereby confirmed by the zeta potential behavior as a function of pH.

Average number of molecules per nanoparticle: NMR Quantification: In order to perform a comparative biological study between the two nanoplatforms, it is necessary to estimate the average number of grafted molecules on the nanoparticle surface. For this, we used the method described in materials and methods (2.3.4). Briefly, after chemical decomposition of the magnetic γFe_2O_3 nanocrystals in acidic medium, the supernatant containing free molecules is analyzed with ^{31}P NMR. An average number of 1200 (± 150) and 4200 (± 250) molecules per nanoparticle is obtained for γFe_2O_3@alendronate and γFe_2O_3@alendronate-PEG nanoparticles respectively. Such difference in surface coverage density could be due to higher steric hindrance provided by amine terminal end group with alendronate compared to hydroxyl end group of alendronate-PEG.

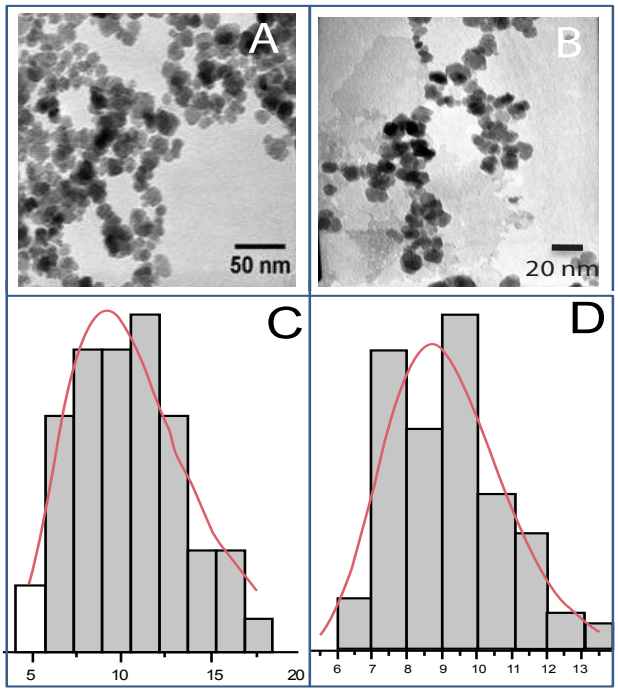

Figure 4: TEM micrograph and size distribution of γFe_2O_3@alendronate (A and C) and of γFe_2O_3@alendronate-PEG (B and D) nanocrystals.

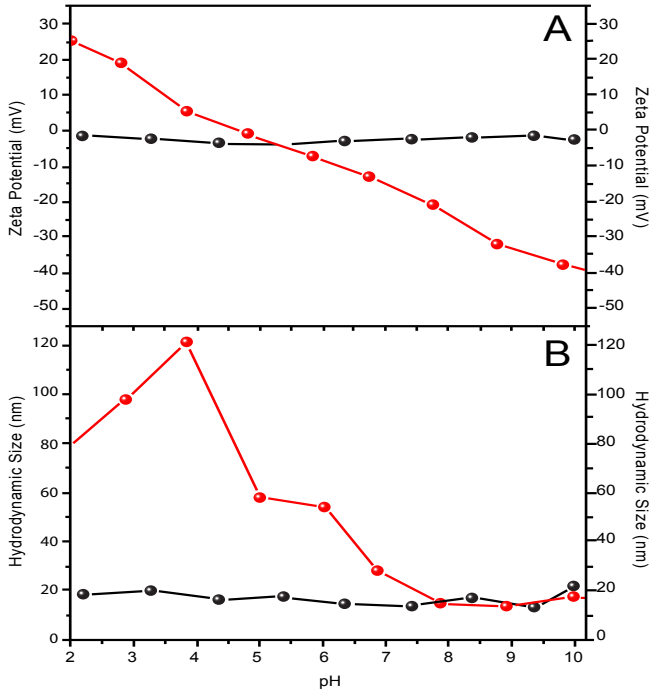

Figure 5: (A) pH-dependent zeta potential and pH-dependent hydrodynamic size curves for γFe_2O_3@alendronate (red) and γFe_2O_3@alendronate-PEG (black) nanocrystals.

In vitro cytotoxicity measurement: The anti-cancerous activity of free molecules and coated nanocrystals was evaluated *in vitro* using HUVEC (Human umbilical vein endothelial cells) as human normal cells and MDA-MB-231 breast human as cancer cell line (Figure 8).

Dose–response curves were obtained for all suspensions allowing the determination of IC_{50} values, which refer to the concentration inducing 50% growth inhibition. Table 2 summarizes all the cytotoxicity results.

From the results in Table 2 and the figure 8, it could be emphasized that free molecules as well as coated nanocrystals do not affect the viability of normal cells (HUVECs). Moreover, it is clear that cytotoxicity of alendronate on MDA-MB-231 cells is reduced by addition of PEG chain. In particular, the IC_{50} value increases around 3.5 times. The differences in the responses of the cell lines to alendronate may be due to differences in membrane permeability or sensitivity to its mechanism of action. Cancer cells are more permeable than normal cells, which explains the lack of efficiency of the alendronate against HUVEC cells. Grafting the molecules (alendronate and alendronate-PEG) on γ-Fe_2O_3 nanoparticles improves the efficiency. Indeed, the IC_{50} is reduced around 3-4 and 2.5 for alendronate and alendronate-PEG respectively. It is well known that cellular uptake of nanoparticles depends highly upon size and charge of the nanoparticles [22,23]. For example it has been shown with quantum dots (QD) that nearly neutral nanoparticle with hydroxyl (-OH) surface functionalization, exhibit greatly reduced non-specific internalization[24], when compared with the carboxyl or amino counterparts, so charge is of a definitive importance to understand the internalization characteristics. While the uptake

mechanisms of nanoparticles into cells is defined as non-specific, these pathways are initiated by surface receptors, either through direct interactions between the charged nanoparticle and the receptor or via proteins adsorbed on the nanoparticles surface. It has been shown that the presence of PEG layer on the nanoparticle surface induced steric hindrance by physically separating the surface from that of the cell (steric hindrance), hence reducing nanoparticle adherence to the cell membrane and leading to reduced internalization. PEG also acts efficiently to reduce protein adsorption onto the nanoparticle surface [22-25]. This property has been shown to prevent phagocytosis, as well as reducing the binding of nanoparticles to the cell membrane, and hence lowering internalization. As can be seen, γFe_2O_3@alendronate-PEG nanoparticles had zeta potentials closer to zero compared to negatively γFe_2O_3@alendronate- charge surface. The difference in the IC_{50} values between pegylated and non pegylated nanoparticles could be attributed to charge effect and reduced cellular uptake with γFe_2O_3@ alendronate-PEG nanoparticles.

Conclusion

In this paper, alendronate-PEG-modified iron oxide nanoparticles about 15 nm in hydrodynamical size have been prepared using one step surface functionalization method and characterized by various physic-chemical means. The colloidal solution of nanoparticles presents high stability on large pH range. In vitro studies show that these nanoparticles exhibit non toxicity on HUVEC cells and anti-tumoral potency on MDAMB-231 breast human cancer cells.

It can be expected that the addition of PEG chains to γFe_2O_3@ alendronate nanoplatform could increase their particle time circulation,

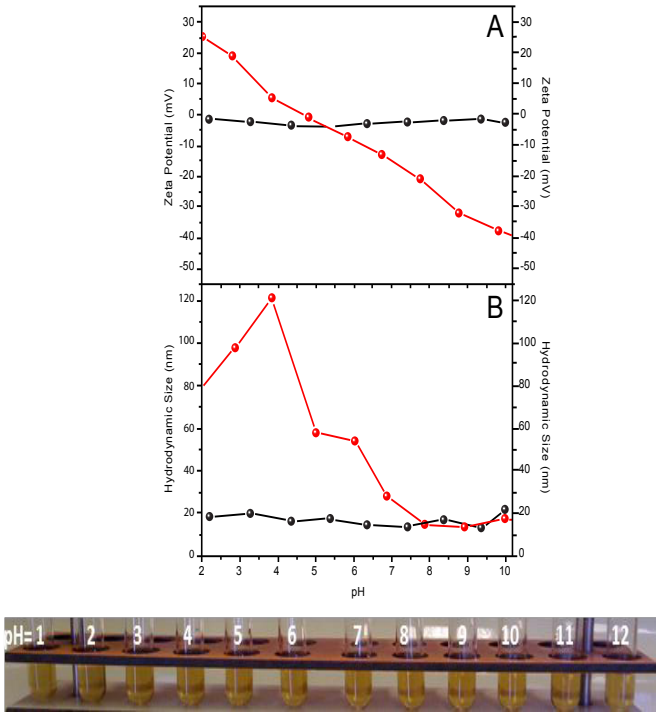

Figure 6: Behaviour of the γFe_2O_3@Alendronate-PEG solutions, as function of pH. The initial conditions are at pH 7 and iron concentration of 5×10^{-3} mol L^{-1}. The suspension pH is then adjusted with sodium hydroxide (NaOH) or acidic (HCl) solutions.

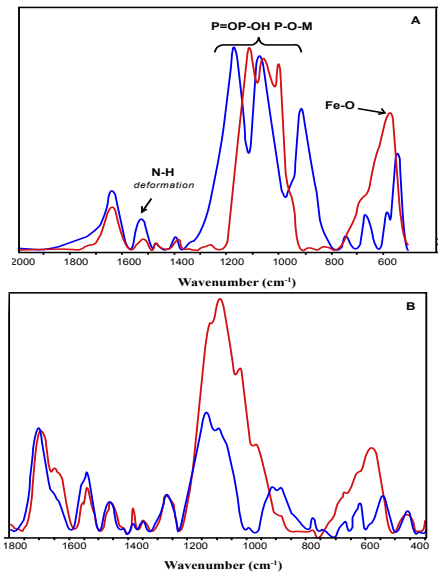

Figure 7: IR spectroscopy in KBr pellets: free molecules (blue curve) and γFe_2O_3 coated nanocrystals (red curve) (A/ Alendronate, B/ Alendronate-PEG).

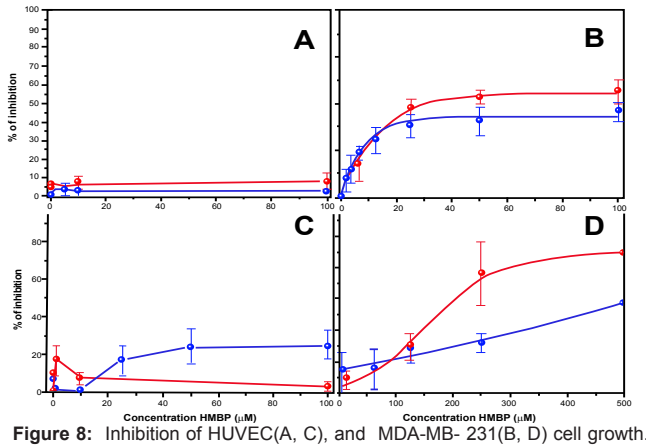

Figure 8: Inhibition of HUVEC(A, C), and MDA-MB- 231(B, D) cell growth. Red plot: free molecules, Blue plot: γFe_2O_3@alendronate (A, B), γFe_2O_3@ alendronate-PEG(C, D).

Cell type	HUVE C		MDA-MB-231	
	IC_{50} (µM)	Growth inhibition maximum (%)	IC_{50} (µM)	Growth inhibition maximum (%)
Free alendronate	-	8	120	50
γ-Fe_2O_3@alendronate nanocrystals	-	8	32	27
Free Alendronate-PEG	-	20	425	58
γ-Fe_2O_3@alendronate nanocrystals	-	10	175	87

Table 2: Half maximal inhibitory concentration (IC50) and maximum percentage of cell inhibition (% Imax) for free Alendronate, γFe_2O_3@alendronate nanocrystals, free Alendronate-PEG and γFe_2O_3@alendronate-PEG nanocrystals with HUVEC, and MDA-MB-231 cell lines.

reduce immunogenicity, and also promotes their accumulation in tumors due to enhanced permeability and retention effect. The terminal OH group of PEG may be selectively oxidized to functionalize PEG with various terminal end groups such as targeting biomolecules

or fluorofores [26]. The effectiveness of this new antitumoral nanoplatform has to be effectively evaluated in vivo.

Supporting information

Synthesis of (4-Amino-1-hydroxy-1-phosphonobutyl) phosphonic acid (Alendronate): Alendronate was synthesized according to the general procedure [1] for Aminobisphosphonate molecules (BPs) and characterized by ^{1}H and ^{31}P NMR. Briefly, BP was prepared from the corresponding carboxylic acid precursor 4-aminobutyric acid as followed. Carboxylic acid (150 mmol) and H_3PO_3 (150 mmol) were introduced in a three-necked round-bottom flask under inert atmosphere followed by 30 ml of methanesulfonic acid. After heating at 65°C for 1 h, PCl_3 (40 mmol) was slowly added and the reaction was allowed to proceed overnight at 65°C. The resulting yellow viscous reaction mixture was cooled to room temperature, quenched with 500 ml of ice-cold water. The pH was adjusted to 4.3 with a NaOH aqueous solution (0.5 M) and the obtained white precipitate was collected by filtration. This solid was washed five times with a mixture of methanol/water (95:5), dialyzed for 3 days and freeze-dried to finally obtain Alendronate as a sodium salt.

Yield: 82%

I.R. (cm^{-1}): (KBr): 1540, 1172, 1052 cm^{-1}

RMN ^{31}P $\{^{1}H\}$ (80.9 MHz, H_3PO_4/D_2O): 18.5

RMN ^{1}H (500 MHz, D_2O): 3.05 (m, 2H), 2.017 (m, 4H).

Stock solution was prepared at 10 mM in deionized water. Dilutions of the stock solution were conducted with Eagle's medium, and the highest tested concentration corresponded to 1 mM.

Synthesis of 2-{2-[2-(2-Benzyloxy-ethoxy)-ethoxy]-ethoxy}-ethanol 2: Sodium hydride (50 mmol, 1 eq.) was introduced in a three-necked flask, in 50 mL of dry THF with stirring under inert atmosphere. Polyethylene glycol 200 (50 mmol, 1 eq.) was added drop wise and at 0°C. The reaction mixture thus obtained was stirred and refluxed for 1h 30 in absence of light. 8.55 g of benzyl bromide (50 mmol, 1 eq.) was then added drop wise at room temperature. The evolution of the reaction was monitored by TLC with dichloromethane-ethanol (9/1) as eluent. Once completed, the reaction mixture NaBr salts was filtered. The recovered filtrate was then dried over anhydrous $MgSO_4$, filtrated and evaporated under reduced pressure. A brown oil was obtain and purified by chromatography column on silica using dichloromethane - ethanol (95/5) as eluent.

Yield: 70%

I.R. (cm^{-1}) : 940, 1100, 1249, 1351, 1453, 2867, 3453

RMN ^{1}H (200 MHz, $CDCl_3$): 2.54 (s, 2H), 3.66 (m, 14H), 4.56 (s, 2H), 7.32 (s, 5H)

Synthesis of Imidazole-1-carboxylique 2-{2-[2-(2-benzyloxy-ethoxy)-ethoxy]-ethoxy}-ethyl ester 3: Carbodiimidazole (CDI) (30.8 mmol, 1.1 eq.) was dissolved, under inert atmosphere, in 40 mL of previously distilled acetonitrile. After several minutes of stirring, alcohol **2** (28 mmol, 1 eq.) was added dropwise at 0°C, the reaction mixture was placed in an ice bath. The solution was yellow. After 15 minutes of stirring, the mixture was cooled to room temperature; the reaction progress was followed by TLC with dichloromethane-ethanol (9/1) as eluent. Once completed, the reaction mixture was then filtered. The filtrate recovered was then dried over anhydrous $MgSO_4$ and evaporated under reduced pressure. A brown oil was recovered obtain . The resulting desired activated alcohol was immediately engaged in the following reaction without further purification.

I.R. (cm^{-1}): 754, 1099, 1290, 1763, 2869

RMN ^{1}H (200 MHz, $CDCl_3$): 3.60 (m, 12H), 4.50 (s, 2H), 6.98 (s, 2H), 7.28 (s, 5H), 7.65 (s, 1H)

Synthesis of [4-(2-{2-[2-(2-Benzyloxy-ethoxy)-ethoxy]-ethoxy}-ethoxycarbonylamino)-1-hydroxy-1-phosphono-butyl]-phosphonic acid 4: In a 500 mL flask, protected from light, previously obtained activated alcohol **3** (19.14 mmol, 2 eq.) was dissolved in 20 mL of dry dichloromethane at room temperature. After several minutes of stirring, alendronate (9.57 mmol, 1 eq.) dissolved in 20 mL of water was added drop wise. The solution of alendronate was previously set to pH 12. The evolution of the reaction was monitored by ^{31}P NMR. Once completed, the two phases were separated. The aqueous phase was evaporated. The white obtained solid was precipitated in 50 mL of acetone. It was purified by reverse phase chromatography column using water - methanol (95/5) as eluent.

Yield: 80%

RMN ^{1}H (200 MHz, D_2O): 1.9 (m, 4H), 3.20 (t, 2H), 3.75 (m, 14H), 4.19 (s, 2H), 4.66 (s, 2H), 7.31 (s, 5H)

RMN ^{31}P $\{^{1}H\}$ (80.9 MHz, H_3PO_4/D_2O): 18.90 (s)

MS: ($C_{20}H_{35}NO_{13}P_2$) m/z: [M + Na]+ = 582,16 ; [M + 2Na - H]+ = 604,14 ; [M + 3Na -2H]+ = 626,11; calc: 559.

Synthesis o [1-Hydroxy-4-(2-{2-[2-(2-hydroxy-ethoxy)-ethoxy]-ethoxy}- ethoxycarbonylamino)-1-phosphono-butyl]-phosphonic acid 5: Protected Alendronate-PEG **4** was dissolved in 5.4 mL of deionised water. 0.06 g of palladium on charcoal 10% (30% by weight) was added with stirring. Air was replaced by hydrogen. After 24 hours stirring, the reaction was complete. The solution was centrifuged and the supernatant was lyophilized to obtain a white powder.

Yield: 80%

RMN ^{1}H (200 MHz, D_2O): 1.87 (m, 2H), 2.10 (m, 2H), 3.16 (t , 2H $^{3}J_{H-H}$ =6.9 Hz), 3.72 (m, 14H), 4.21(s, 2H)

I.R. (cm^{-1}): 541, 1139, 1268, 1701, 2923

RMN ^{31}P $\{^{1}H\}$ (80.9 MHz, H_3PO_4/D_2O): 18.13 (s)

MS: ($C_{13}H_{29}NO_{13}P_2$) m/z: $[M + H]^+$ = 470,42; calc: 469.

References

1. Benyettou F, Lalatonne Y, Chebbi I, Di Benedetto M, Serfaty JM, et al. (2011) Multimodal magnetic resonance imaging nanoplatform for cancer theranostics. PCCP 13: 10020–10027.
2. Benyettou F, Chebbi I, Motte L, Seksek O (2011) Magnetoliposome for Alendronate delivery. J Mater Chem 21: 4813-4820.
3. Lalatonne Y, Paris C, Serfaty JM, Weinmann P, Lecouvey M, et al. (2008) Bis-phosphonates–ultra small superparamagnetic iron oxide nanoparticles: a platform towards diagnosis and therapy. Chem Commun 20: 2553–2555.
4. Delgado C, Francis GE, Fisher D (1992) The uses and properties of PEG-linked proteins. Crit Rev Ther Drug Carrier Syst 9: 249-304.
5. Abuchowski A, Van Es T, Palczuk NC, Davis FF (1977) Alteration of immunological properties of bovine serum albumin by covalent attachment of polyethylene glycol. The Journal of Biological Chemistry 252: 3578-3581.
6. Gabizon A, Catane R, Uziely B, Kaufman B, Safra T, et al. (1994) Prolonged

Circulation Time and Enhanced Accumulation in Malignant Exudates of Doxorubicin Encapsulated in Polyethylene-glycol Coated Liposomes. Cancer Res 54: 987.

7. Montet X, Weissleder R, Josephson L (2006) Imaging pancreatic cancer with a peptide-nanoparticle conjugate targeted to normal pancreas. Bioconjug Chem 17: 905-911.
8. Zhu B, Eurell T, Gunawan R, Leckband D (2001) Chain-length dependence of the protein and cell resistance of oligo(ethylene glycol)-terminated self-assembled monolayers on gold. J Biomed Mater Res 56: 406-416.
9. Park KD, Kim YS, Han DK, Kim YH, Lee EHB, et al. (1998) Bacterial adhesion on PEG modified polyurethane surfaces. Biomaterials 19: 851-859.
10. Harris JM (1992) Synthesis of New Poly(Ethy1ene Glycol) Derivatives. In Poly (ethylene glycol) Chemistry: Biotechnical and Biomedical Applications (Harris JM Ed.) 347-370 Plenum Press, New York.
11. Veronese FM, Pasut G (2005) PEGylation, successful approach to drug delivery. Drug Discov Today 10: 1451–1458.
12. Stolnik S, Illum L, Davis SS (1995) Long circulating microparticulate drug carriers. Adv Drug Deliv Rev 16: 195-214.
13. Wanga M, Thanoua M (2010) Targeting nanoparticles to cancer. Pharmacol Res 62: 90-99.
14. Bechet D, Couleaud P, Frochot C, Viriot ML, Guillemin F, et al.(2008) Nanoparticles as vehicles for delivery of photodynamic therapy agents. Trends in Biotechnology 26: 612-621.
15. Joralemon MJ, McRae S, Emrick T (2010) PEGylated polymers for medicine: from conjugation to self-assembled systems. Chem Commun 46: 1377-1393.
16. Sun LY, Han J, He J, Zhonggui (2010) Long-circulating Targeted Nanoparticles for Cancer Therapy Current Nanoscience 6: 347-354.
17. Motte L, Benyettou F, de Beaucorps C, Lecouvey M, Milesovic I, et al. (2011) Multimodal superparamagnetic nanoplatform for clinical applications: immunoassays, imaging & therapy. Faraday Discuss 149: 211-225.
18. Benyettou F, Lalatonne Y, Sainte-Catherine O, Monteil M, Motte L (2009) Superparamagnetic nanovector with anti-cancer properties: γFe2O3@ Zoledronate. Int J Pharm 379: 324-327.
19. Katsumi H, Yamamoto A, Nakatani M, US patent 2008, 0182823.
20. Simões S, Filipe A, Faneca H, Mano M, Penacho N, et al. (2005) Cationic liposomes for gene delivery. 2: 237-254.
21. Shakyaa AK, Sami H, Srivastavaa A, Kumar A (2010) Stability of responsive polymer–protein bioconjugates. Progress in Polymer Science 35: 459-486.
22. Mornet S, Vasseur S, Grasset F, Duguet E (2004) Magnetic nanoparticle design for medical diagnosis and therapy. J Mater Chem 14: 2161-2175.
23. Kelf TA, Sreenivasan VKA, Sun J, Kim EJ , Goldys EM, et al. (2010) Non-specific cellular uptake of surface-functionalized quantum dots. Nanotechnology 21: 285105 .
24. Kairdolf BA, Mancini MC, Smith AM, Nie S (2008) Minimizing nonspecific cellular binding of quantum dots with hydroxyl-derivatized surface coatings. Anal Chem 80**:** 3029-3034.
25. Vonarbourg A, Passirani C, Saulnier P, Benoit JP (2006) Parameters influencing the stealthiness of colloidal drug delivery systems. Biomaterials 27: 4356-4373.
26. Benyettou F, Guenin E, Lalatonne Y, Motte L (2011) Microwave assisted nanoparticle surface functionalization. Nanotechnology 22: 1-7.